

## Supporting Information

# Zero-dimensional Hybrid Lead Perovskite with Highly Efficient Blue-Violet Light Emission

Chen Sun,<sup>a,b</sup> Kuan Jiang,<sup>a</sup> Meng-Fei Han,<sup>a</sup> Mei-Jun Liu,<sup>a</sup> Xi-Kai Lian,<sup>a</sup> Yong-Xin Jiang,<sup>a</sup> Hua-Sen Shi,<sup>a</sup> Cheng-Yang Yue,<sup>a\*</sup> Xiao-Wu Lei<sup>a\*</sup>

<sup>a</sup>Department of Chemistry and Chemical Engineering, Jining University, Qufu, Shandong, 273155, P. R. China

<sup>b</sup>College of Chemistry and Chemical Engineering, Qufu Normal University, Qufu, Shandong, 273165, P. R. China

\*Corresponding author: Cheng-Yang Yue, Xiao-Wu Lei

E-mail address:yuechengyang@126.com; xwlei\_jnu@163.com

## Experimental Section

**Materials and characterizations.** All the chemical reagents were commercially purchased from Aladdin chemical company and directly used in the preparation reaction without any further purification or other physical process. PbCl<sub>2</sub> (99.9%), N,N'-Bis(3-aminopropyl)-ethylenediamine (BAPrEDA, 97%), isopropyl alcohol (99%) and hydrochloric acid (HCl, 37%). The powder X-ray diffraction experiments were performed on a Bruker D8 Advance X-ray powder diffraction meter operating at 40 kV and 40 mA (Cu- $K_{\alpha}$  radiation,  $\lambda = 1.5418 \text{ \AA}$ ). The solid state UV-Vis absorption optical spectra for powder sample were collected at PE Lambda 900 UV/Vis spectrophotometer at room temperature in wavelength range of 200–800 nm. The thermogravimetric analysis (TGA) was carried out on a Mettler TGA/SDTA 851 thermal analyzer from room temperature to 800°C under the flow of nitrogen atmosphere. Elemental analyses of C, N and H were carried out on a PE2400 II elemental analyzer.

**Synthesis of compound [BAPrEDA]PbCl<sub>6</sub>·(H<sub>2</sub>O)<sub>2</sub>(1).** The mixture of PbCl<sub>2</sub>(0.4 mmol, 0.1112 g) and 0.1 mmol N,N'-Bis(3-aminopropyl)-ethylenediamine (BAPrEDA, 0.7 mmol, 0.119 g) were dissolved in mixed solution of isopropyl alcohol (1 mL) and hydrochloric acid (5 mL, 34%), and the mixture was stirred for 20 minutes until the uniformity at room temperature, and then the solution was sealed in a 25 mL Teflon liner fixed by stainless steel reactor. The mixture was heated at constant temperature of 180 °C for at least five days, and subsequently cooled to room temperature with controlled cooling rate of 5 °C·min<sup>-1</sup>. A lot of colorless prism crystals were filtrated and washed using ethanol in yield of 61% (calculation based on PbCl<sub>2</sub>), and subsequently determined to be [BAPrEDA]PbCl<sub>6</sub>·(H<sub>2</sub>O)<sub>2</sub>(1) based on single crystal X-ray diffraction. Elemental analysis calculated for C<sub>8</sub>H<sub>30</sub>N<sub>4</sub>O<sub>2</sub>PbCl<sub>6</sub>: C, 15.15 %; N, 8.83 %; H, 4.77%; found: C, 15.23 %; N,

8.75%; H, 4.69 %.

**X-ray Crystallography.** The single crystal data of compound **1** was collected on the Bruker Apex II CCD diffractometer with Mo K $\alpha$  radiation ( $\lambda = 0.71073 \text{ \AA}$ ) at room temperature. The crystal structures were solved by direct method and refined based on  $F^2$  using SHELXTL-97 program. All the non-hydrogen atoms were refined with anisotropic thermal parameters, and hydrogen atoms of organic molecules were positioned geometrically and refined isotropically. Structural refinement parameters of compound **1** are summarized in Table S3 and important bond lengths are listed in Table S4-S5.

**Photoluminescence property characterization.** The PL spectra were performed on an Edinbergh FLS980 fluorescence spectrometer. The photoluminescence quantum efficiency (PLQE) was achieved by incorporating an integrating sphere into the FLS980 spectro fluorometer. The PLQE was calculated based on the equation:  $\eta_{\text{QE}} = I_{\text{S}}/(E_{\text{R}} - E_{\text{S}})$ , which  $I_{\text{S}}$  represents the luminescence emission spectrum of the sample,  $E_{\text{R}}$  is the spectrum of the excitation light from the empty integrated sphere (without the sample), and  $E_{\text{S}}$  is the excitation spectrum for exciting the sample. The time-resolved decay data were carried out using the Edinburgh FLS980 fluorescence spectrometer with a picosecond pulsed diode laser. The average lifetime was obtained by exponential fitting. The power-dependent photoluminescence spectra were measured using the 375 nm (LE-LS-375-140TFCA, 1-140 mW). The CIE chromaticity coordinates and CRI were calculated using the CIE calculator software based on the emission spectrum.

**Theoretical band calculation.** The single crystal data of compound **1** was directly used to calculate the electronic band structure in Castep software. The total energy was calculated with density functional theory (DFT) using Perdew–Burke–Ernzerhof (PBE) generalized gradient

approximation. The interactions between the ionic cores and the electrons were described by the norm-conserving pseudo potential. Hence, the C- $2s^22p^2$ , N- $2s^22p^3$ , H- $1s^1$ , Pb- $6s^26p^2$  and Cl- $3s^2sp^5$ orbital were adopted as valence electrons. The number of plane wave included in the basis sets was determined by a cutoff energy of 340 eV and numerical integration of the Brillouin zone is performed using Monkhorst-Pack k-point sampling of  $2\times2\times2$ . Other calculating parameters and convergence criteria were set by the default values of the CASTEP code.

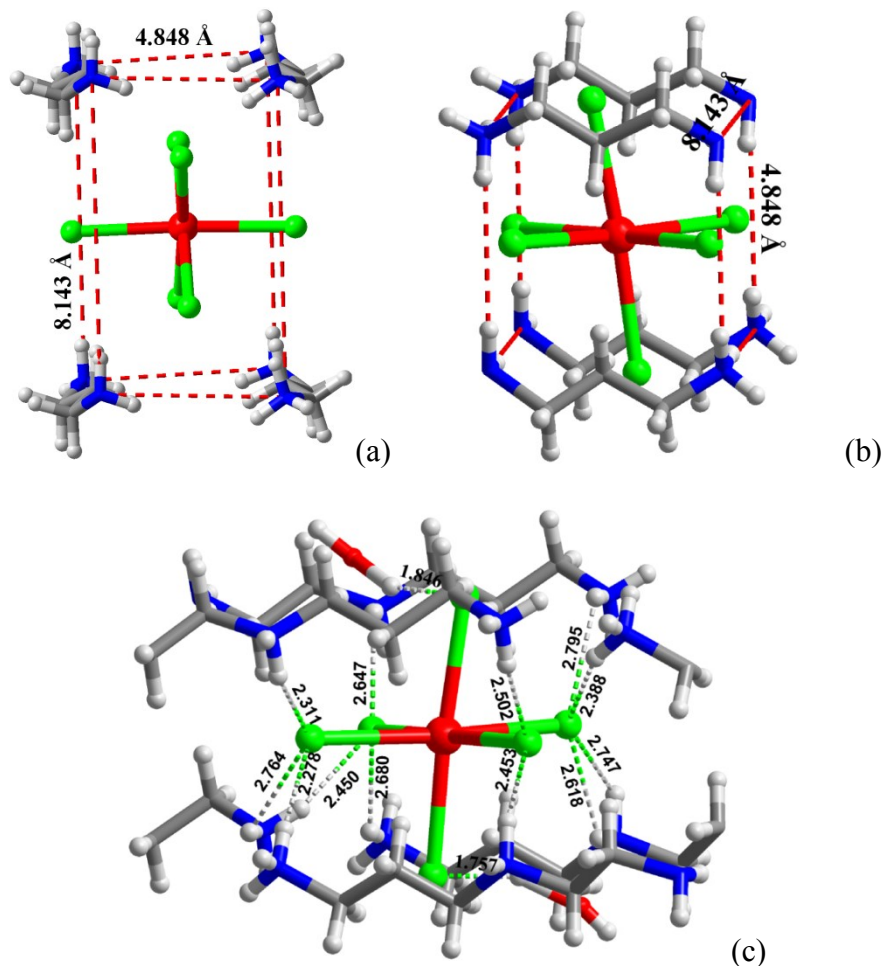


**Fig. S1.** The detailed view of the confined environment around  $[\text{PbCl}_6]^{4-}$  unit (a and b), and the hydrogen bonding interactions between  $[\text{PbCl}_6]^{4-}$  unit and organic cations in compound **1** (c).

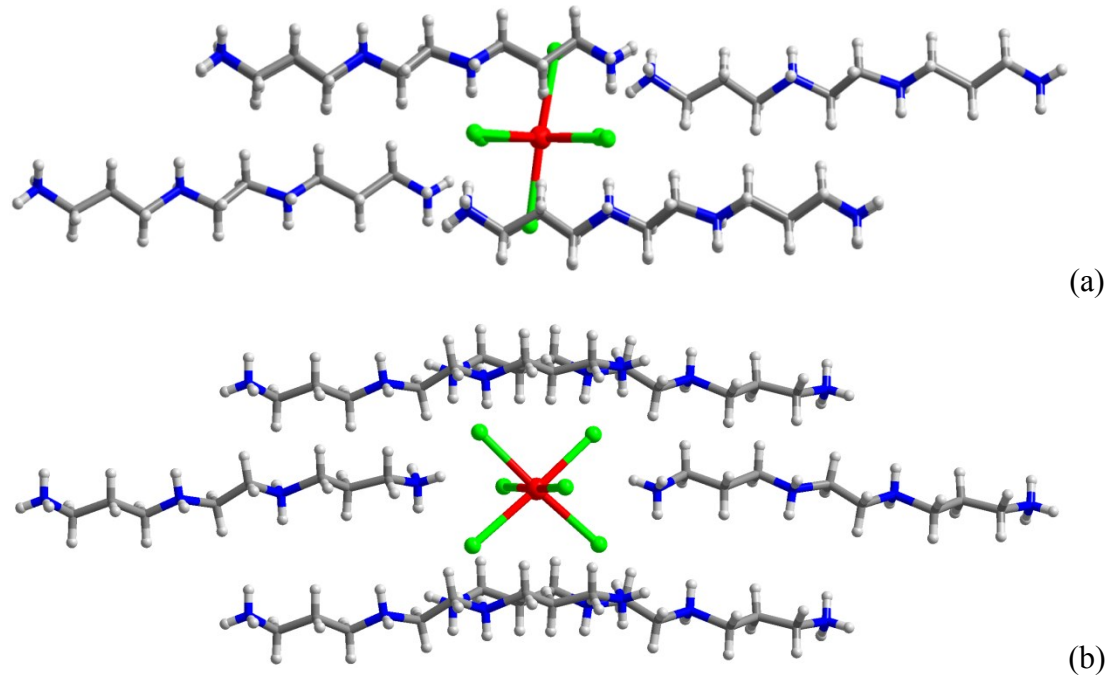


**Fig. S2.** View of the  $[PbCl_6]^{4-}$  unit embedding in the organic matrix along the *b*-axis (a) and *c*-axis (b) in compound **1**.

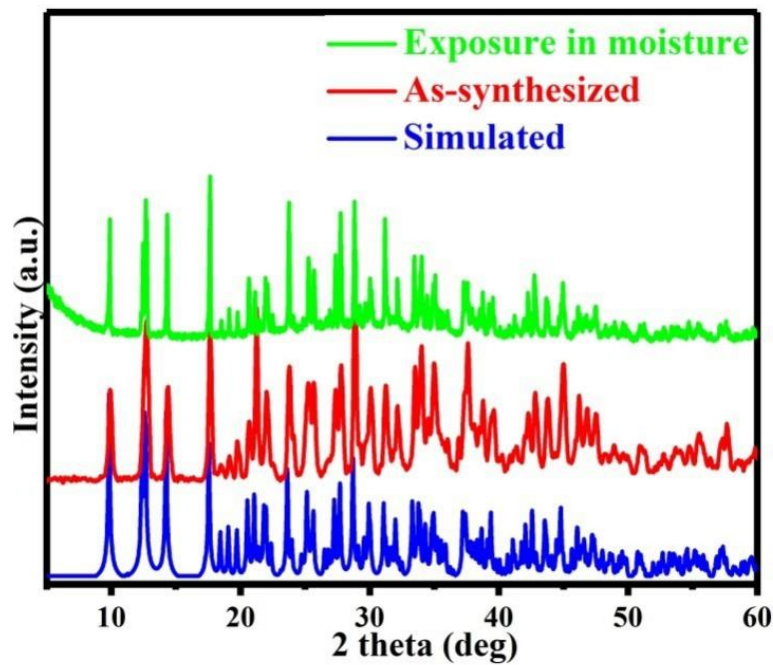


**Fig. S3.** The simulated and experimental XRD patterns of as-synthesized compound **1** as well as after exposure in moisture air for about 4 months.

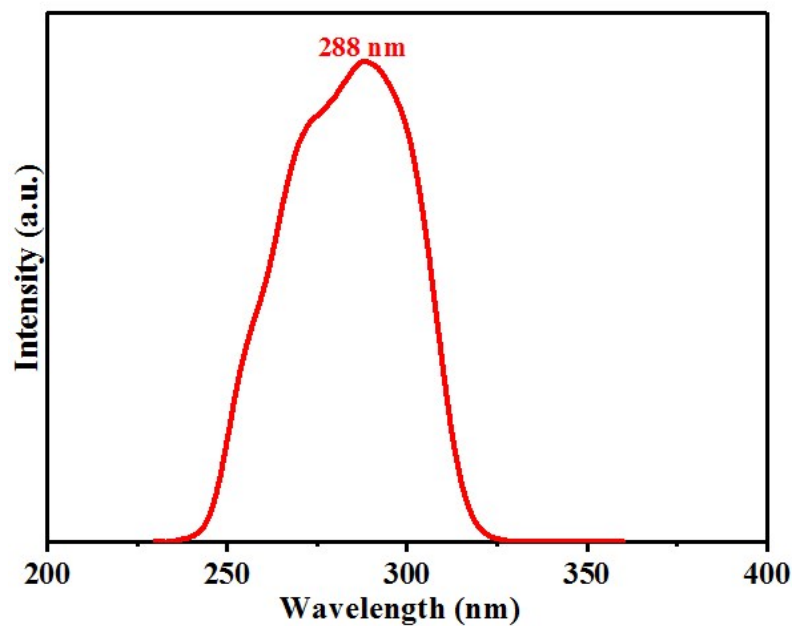


**Fig. S4.** The PL excitation spectrum of compound **1** at room temperature.

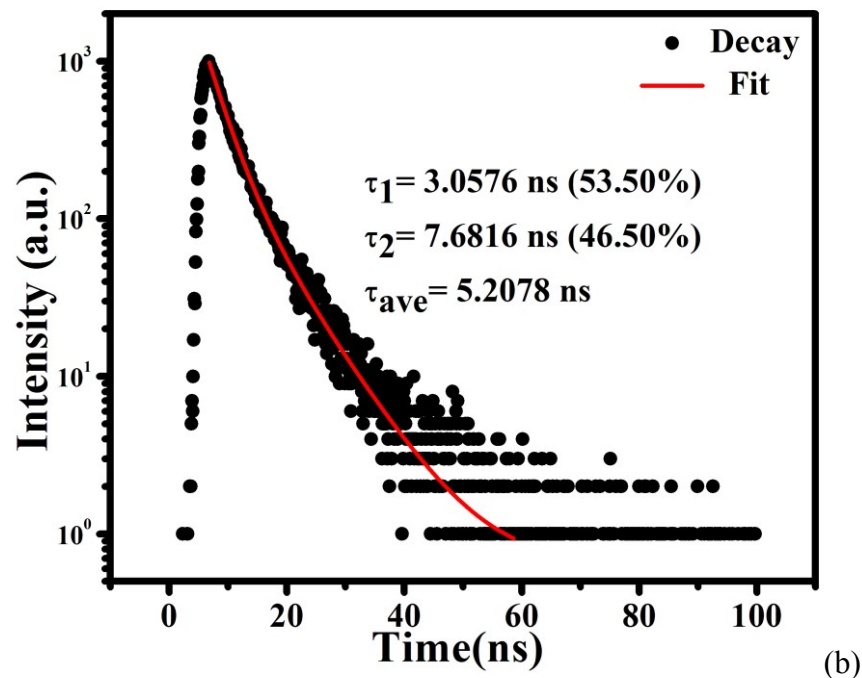
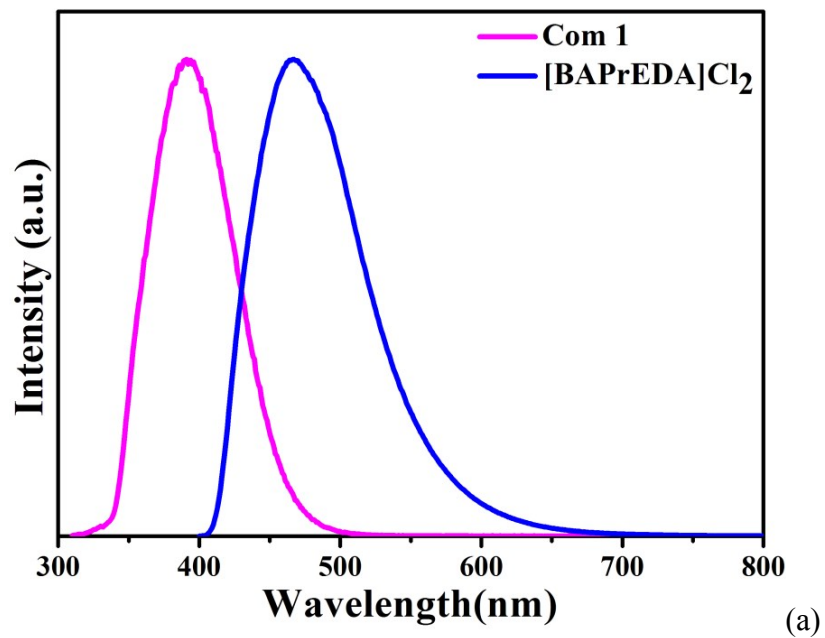


**Fig. S5.** (a) Comparison of PL emission spectra of compound **1** and  $[\text{BAPrEDA}]\text{Cl}_2$ , (b) the time-resolved PL decay curve of  $[\text{BAPrEDA}]\text{Cl}_2$ .

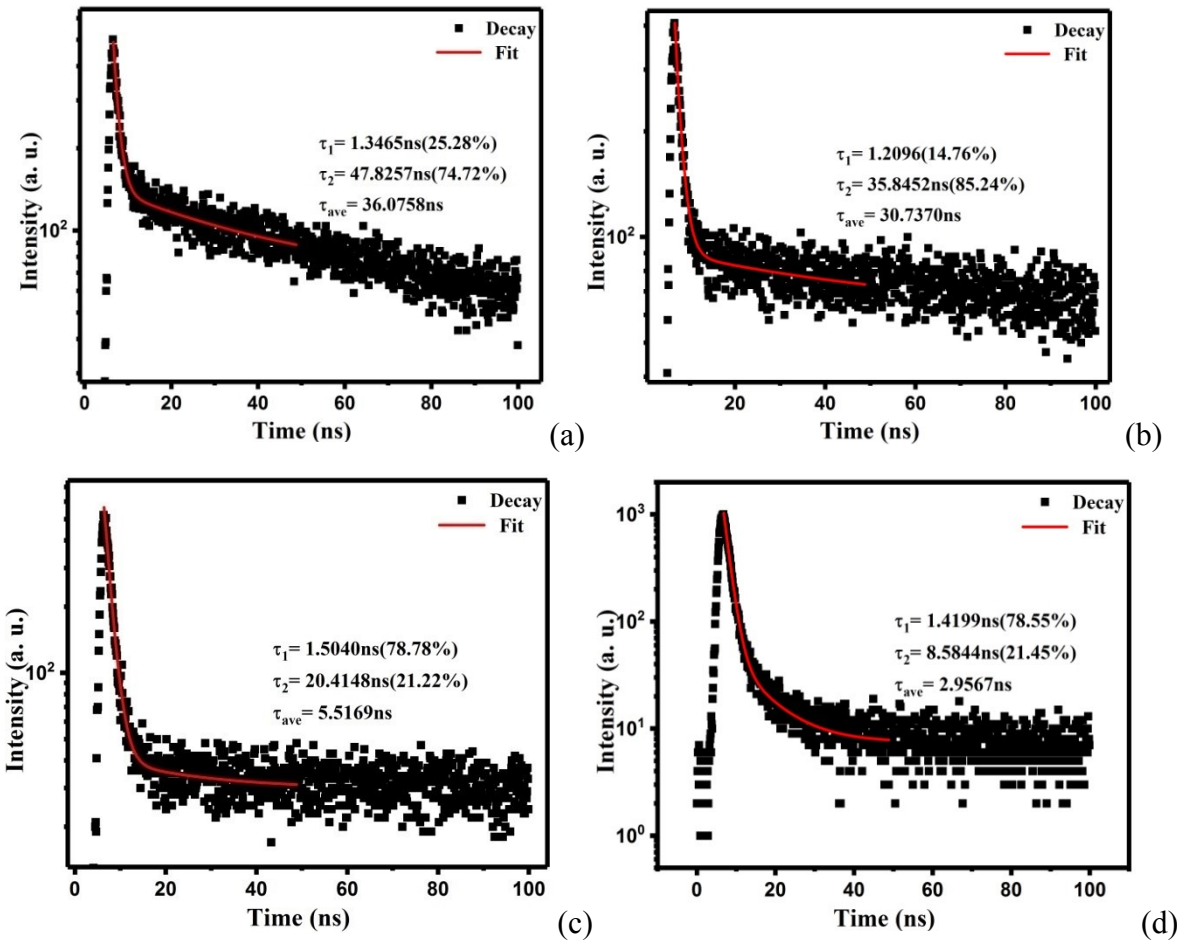


**Fig. S6.** The time-resolved PL decay curve (measured at 392 nm) at 260 K (a), 200K (b), 140K (c) and 80K (d).

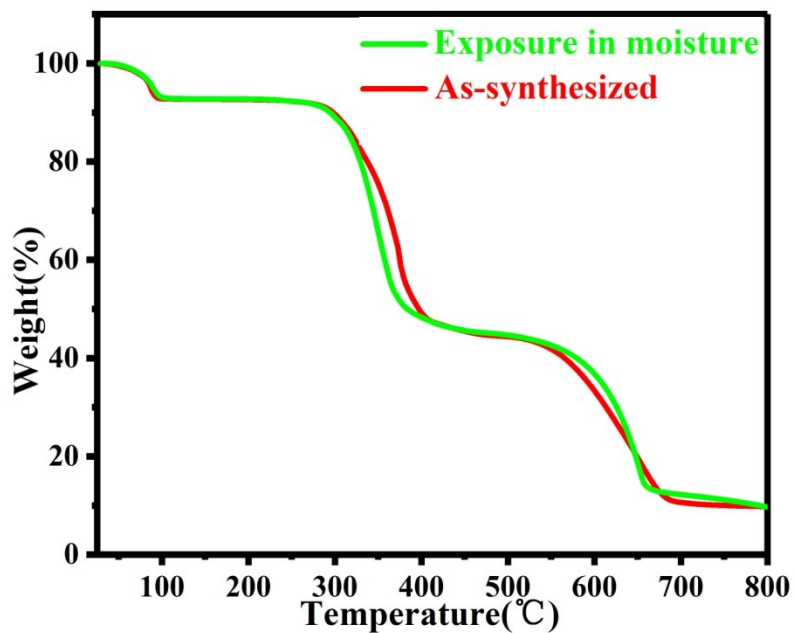


**Fig. S7.** The thermogravimetric analyses curves for as-synthesized compound **1** as well as after exposure in moisture air for about 4 months. The first step of losing weight corresponds to the dehydration process and the residual [BAPrEDA]PbCl<sub>6</sub> component can be stable up to about 300 °C.

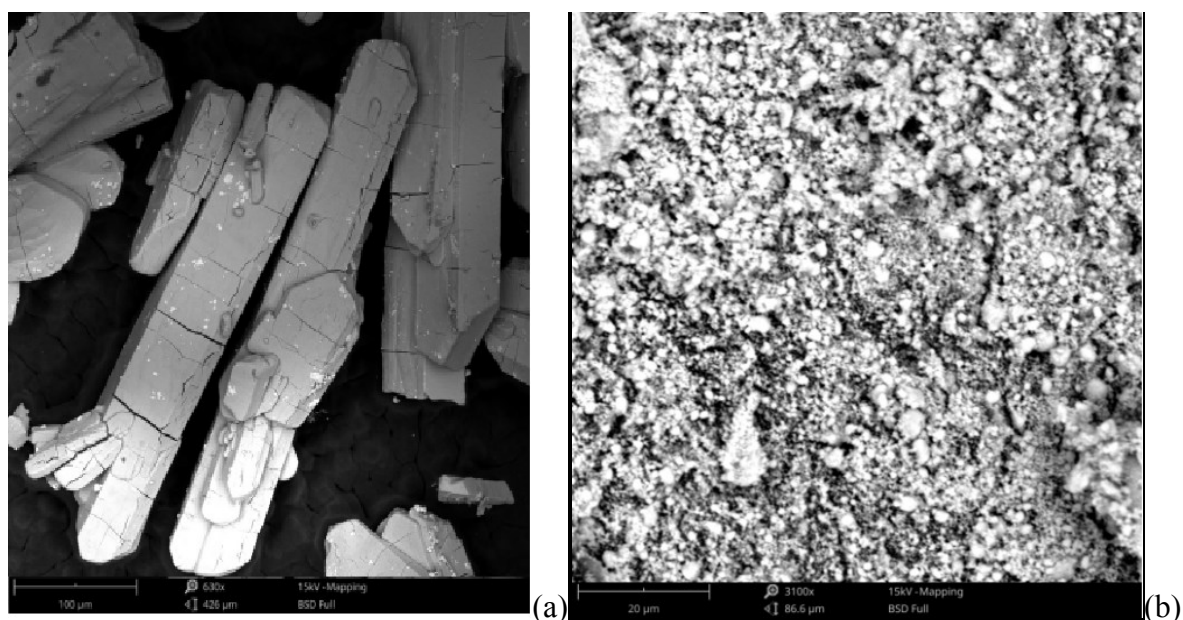


**Fig. S8.** The SEM photos of bulk crystals and grinded microscale powders for compound **1**.

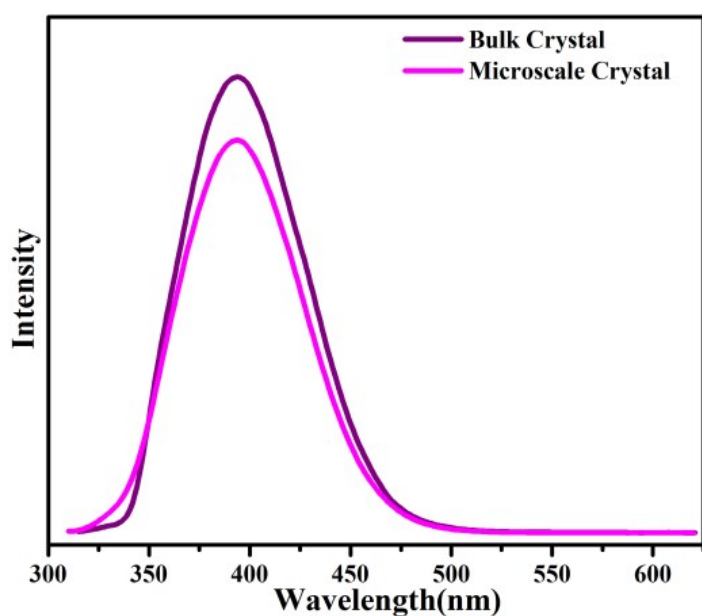


**Fig. S9.** Photoluminescence spectra of bulk crystals and grinded microscale powders for compound 1measured at room temperature.

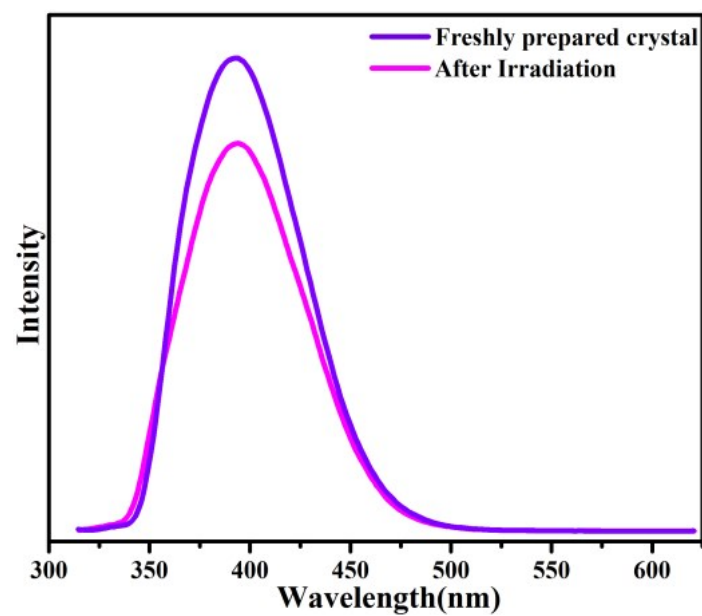


**Fig. S10.** PL emission spectra of bulk crystals before and after UV light irradiation of 24 hour for compound 1measured at room temperature.

**Table S1.** Comparison of the PL excitations and emissions as well as the Stokes shifts in single crystalline 0D metal halides.

Compound	Excitation	Emission	Stocks Shift	Ref
[BAPrEDA]PbCl <sub>6</sub> ·(H <sub>2</sub> O) <sub>2</sub>	<b>300 nm (4.13 eV)</b>	<b>392 nm (3.16 eV)</b>	<b>92 nm (0.97 eV)</b>	<b>This work</b>
(C <sub>13</sub> H <sub>19</sub> N <sub>4</sub> ) <sub>2</sub> PbBr <sub>4</sub>	349 nm (3.55 eV)	460 nm (2.70 eV)	111 nm (0.85 eV)	1
(Bmpip <sub>2</sub> )PbBr <sub>4</sub>	347 nm (3.57 eV)	470 nm (2.64 eV)	123 nm (0.93 eV)	2
(btmpy) <sub>7</sub> [PbCl <sub>4</sub> ][Pb <sub>3</sub> Cl <sub>11</sub> ]	348 nm (3.56 eV)	470 nm (2.64 eV)	122 nm (0.92eV)	3
(C <sub>9</sub> NH <sub>20</sub> ) <sub>2</sub> SnBr <sub>4</sub>	365 nm (3.40 eV)	695 nm (1.78 eV)	332 nm (1.62 eV)	4
(C <sub>4</sub> N <sub>2</sub> H <sub>14</sub> Br) <sub>4</sub> SnBr <sub>6</sub>	355 nm (3.49 eV)	570 nm (2.18 eV)	215 nm (1.31 eV)	5
(C <sub>9</sub> NH <sub>20</sub> ) <sub>2</sub> SbCl <sub>5</sub>	380 nm(3.26 eV)	590 nm(2.10 eV)	210 nm(1.16 eV)	6
(C <sub>4</sub> N <sub>2</sub> H <sub>14</sub> I) <sub>4</sub> SnI <sub>6</sub>	410 nm(3.02 eV)	620 nm(2.00 eV)	210 nm(1.02 eV)	7
(Bmpip <sub>2</sub> )GeBr <sub>4</sub>	340 nm (3.65 eV)	670 nm(1.85 eV)	330 nm(1.80 eV)	2
(Bmpip <sub>2</sub> )SnBr <sub>4</sub>	340 nm (3.65 eV)	666 nm(1.86 eV)	326 nm(1.79 eV)	2
(Bmpip <sub>2</sub> )SnI <sub>4</sub>	410 nm(3.02 eV)	730 nm(1.70 eV)	360 nm(1.32 eV)	2
(Ph <sub>4</sub> P) <sub>2</sub> SbCl <sub>5</sub>	375 nm(3.31 eV)	648 nm(1.91 eV)	273 nm(1.40 eV)	8
(btmpy) <sub>9</sub> [ZnBr <sub>4</sub> ] <sub>2</sub> [Pb <sub>3</sub> Br <sub>11</sub> ]	379 nm (3.79 eV)	564 nm(2.20 eV)	185 nm(1.59 eV)	9
(PMA) <sub>3</sub> InBr <sub>6</sub>	365 nm(3.40 eV)	610 nm(2.03 eV)	245 nm(1.37 eV)	10
(C <sub>4</sub> H <sub>14</sub> N <sub>2</sub> ) <sub>2</sub> In <sub>2</sub> Br <sub>10</sub>	365 nm (3.40 eV)	670 nm (1.85 eV)	300 nm (1.55 eV)	11
Cs <sub>2</sub> InBr <sub>5</sub> ·H <sub>2</sub> O	355 nm (3.49 eV)	695 nm (1.78 eV)	340 nm (1.71 eV)	12

**Table S2.** Summary of the Blue-Violet-Emitting Properties (<500nm) of Lead Halide Perovskites.

Phase	Emission (nm)	PLQY (%)	FWHM (nm)	Lifetime (ns)	Ref.
<b>Single Crystalline lead halides</b>					
[BAPrEDA]PbCl <sub>6</sub> ·(H <sub>2</sub> O) <sub>2</sub>	390	21.28	73	36.64	This work
(C <sub>6</sub> H <sub>5</sub> CH <sub>2</sub> NH <sub>3</sub> ) <sub>2</sub> PbBr <sub>4</sub>	411	60-79	20	-	<i>Nat. Mater.</i> 2018, <b>17</b> , 550
C <sub>5</sub> H <sub>14</sub> N <sub>2</sub> PbCl <sub>4</sub> ·H <sub>2</sub> O	412	1	-	5.6	<i>J. Mater. Chem. C</i> , 2018, <b>6</b> , 6033
(C <sub>13</sub> H <sub>19</sub> N <sub>4</sub> ) <sub>2</sub> PbBr <sub>4</sub>	460	40	66	75	<i>ACS Materials Lett.</i> 2019, <b>1</b> , 594
(Bmpip <sub>2</sub> )PbBr <sub>4</sub>	470	24	-	66	<i>J. Am. Chem. Soc.</i> 2019, <b>141</b> , 9764
(bmpy) <sub>7</sub> [PbCl <sub>4</sub> ][Pb <sub>3</sub> Cl <sub>11</sub> ]	470	83	84	418	<i>J. Am. Chem. Soc.</i> 2018, <b>140</b> , 13181
<b>Perovskite Quantum Dots and Nanomaterials</b>					
Cd@CsPbCl <sub>3</sub> PQD	406	96 ± 2	12	5.30	<i>ACS Energy Lett.</i> 2019, <b>4</b> , 32-39
Ni@CsPbCl <sub>3</sub> PQD	408	96.5	-	18.39	<i>J. Am. Chem. Soc.</i> 2018, <b>140</b> , 9942
Ni@CsPbCl <sub>2</sub> Br PQD	425	93.1	-	10.69	
Ni@CsPbCl <sub>2.4</sub> Br <sub>0.6</sub> PQD	415	92	-	13.74	
Mg@ CsPbCl <sub>3</sub> PQD	403	79	-	3.69	<i>J. Phys. Chem. Lett.</i> 2020, <b>11</b> , 1178
Ca@CsPbCl <sub>3</sub> PQD	406	77.1	-	17.86	<i>Chem. Mater.</i> 2019, <b>31</b> , 3974
CsPbCl <sub>3</sub> PQD	408	65	11	7.7	<i>J. Am. Chem. Soc.</i> 2018, <b>140</b> , 2656
MAPbCl <sub>3</sub>	404	5	15	5.4	
FAPbCl <sub>3</sub>	407	2	16	14.8	
Cu@ CsPbCl <sub>3</sub> PQD	403	60	14	1.43	<i>ACS Materials Lett.</i> 2019, <b>1</b> , 116
CsPbCl <sub>3</sub> PQD	402	50	14	3.82	<i>Chem. Mater.</i> 2018, <b>30</b> , 3633
La@CsPb(Cl <sub>0.7</sub> F <sub>0.3</sub> ) <sub>3</sub> PQD	410	36.5	-	22.9	<i>Nanoscale</i> 2019, <b>11</b> , 2484-2491
CsPbCl <sub>3</sub> PQD	408	34.2	13	8.60	<i>ACS Appl. Mater. Interfaces</i> 2019, <b>11</b> , 14256
Cs <sub>4</sub> PbBr <sub>6</sub> NCs	405	22	66	1.27	<i>J. Phys. Chem. C</i> 2020, <b>124</b> , 1617
CsPbCl <sub>3</sub> NCs	402	1	14	< 65 ps	<i>Chem. Mater.</i> 2018, <b>30</b> , 3633–3637
CsPbCl <sub>2</sub> Br NCs	427	1	-	< 65 ps	
CsPbCl <sub>3</sub> PQD	408	10	12	-	<i>Adv. Funct. Mater.</i> 2016, <b>26</b> , 2435
(PEA) <sub>2</sub> PbBr <sub>4</sub> Nanoplate	407	EQE= 0.04	14	1.27	<i>ACS Nano</i> , 2016, <b>10</b> , 6897

B-MDs-PbBr <sub>4</sub> Nanosheets	403	53	11	4.71	<i>Chem. Commun.</i> 2015, <b>51</b> , 16385
T-MDs-PbBr <sub>4</sub> Nanosheets	413	16	11	3.12	
(C <sub>4</sub> H <sub>9</sub> NH <sub>3</sub> ) <sub>2</sub> PbBr <sub>4</sub> 2D Nanosheets	406	26	-	3.3	<i>Science</i> , 2015, <b>349</b> , 1518

**Table S3.** Crystal data and structural refinements for compound **1**.

chemical formula	C <sub>8</sub> H <sub>30</sub> N <sub>4</sub> O <sub>2</sub> PbCl <sub>6</sub>
fw	634.25
Space group	<i>Cc</i> (NO.9)
<i>a</i> /Å	15.388(7)
<i>b</i> /Å	8.143(4)
<i>c</i> /Å	19.336(9)
$\beta/^\circ$	111.503(5)
<i>V</i> (Å <sup>3</sup> )	2254.1(17)
<i>Z</i>	4
<i>D</i> <sub>calcd</sub> (g·cm <sup>-3</sup> )	1.869
Temp (K)	296(2)
$\mu$ (mm <sup>-1</sup> )	8.202
<i>F</i> (000)	1224
Reflections collected	13022
Unique reflections	5174
Reflections ( <i>I</i> >2σ( <i>I</i> ))	4926
GOF on <i>F</i> <sup>2</sup>	1.006
<i>R</i> <sub>1</sub> , <i>wR</i> <sub>2</sub> ( <i>I</i> >2σ( <i>I</i> )) <sup>a</sup>	0.0310/0.0807
<i>R</i> <sub>1</sub> , <i>wR</i> <sub>2</sub> (all data)	0.0329/0.0817

<sup>a</sup>  $R_1 = \Sigma \|F_0 - |F_c|\| / \Sigma |F_0|$ ,  $wR_2 = [\Sigma (F_0^2 - F_c^2) / \Sigma w(F_0)^2]^{1/2}$

**Table S4.** Selected bond lengths ( $\text{\AA}$ ) and bond angles ( $^\circ$ ) for compound **1**.

Pb(1)-Cl(1)	2.808(7)	Pb(1)-Cl(5)	2.908(11)
Pb(1)-Cl(2)	2.840(7)	Pb(1)-Cl(4)	3.002(7)
Pb(1)-Cl(6)	2.846(9)	Pb(1)-Cl(3)	3.042(7)
Cl(1)-Pb(1)-Cl(2)	92.63(8)	Cl(6)-Pb(1)-Cl(4)	95.8(2)
Cl(1)-Pb(1)-Cl(6)	97.3(2)	Cl(5)-Pb(1)-Cl(4)	88.3(2)
Cl(2)-Pb(1)-Cl(6)	81.8(2)	Cl(1)-Pb(1)-Cl(3)	177.4(3)
Cl(1)-Pb(1)-Cl(5)	83.0(3)	Cl(2)-Pb(1)-Cl(3)	85.1(3)
Cl(2)-Pb(1)-Cl(5)	94.0(2)	Cl(6)-Pb(1)-Cl(3)	83.6(2)
Cl(6)-Pb(1)-Cl(5)	175.8(2)	Cl(5)-Pb(1)-Cl(3)	96.0(3)
Cl(1)-Pb(1)-Cl(4)	83.6(3)	Cl(4)-Pb(1)-Cl(3)	98.81(7)
Cl(2)-Pb(1)-Cl(4)	175.2(3)		

**Table S5.** Hydrogen bonds data for compound **1**.

D-H $\cdots$ A	d(D-H)	d(H $\cdots$ A)	d(D $\cdots$ A)	$\angle$ (DHA)
N(1)-H(1A) $\cdots$ Cl(2)	0.90	2.62	3.1126	115
N(1)-H(1B) $\cdots$ Cl(2)	0.90	2.75	3.1126	106
N(1)-H(1B) $\cdots$ Cl(3)	0.90	2.45	3.2491	148
N(2)-H(2A) $\cdots$ Cl(4)	0.90	2.31	3.1058	147
N(2)-H(2B) $\cdots$ Cl(1)	0.90	2.65	3.2112	122
N(3)-H(3A) $\cdots$ Cl(1)	0.89	2.45	3.2579	151
N(3)-H(3B) $\cdots$ Cl(3)	0.89	2.50	3.3028	150
N(3)-H(3C) $\cdots$ Cl(4)	0.89	2.76	3.2235	113
N(3)-H(3C) $\cdots$ Cl(2)	0.89	2.80	3.2485	113
N(4)-H(4A) $\cdots$ Cl(2)	0.89	2.39	3.1941	151
N(4)-H(4B) $\cdots$ Cl(1)	0.89	2.68	3.3865	137
N(4)-H(4C) $\cdots$ Cl(4)	0.89	2.28	3.1646	174

## References

1. H. R. Lin, C. K. Zhou, M. Chaaban, L. J. Xu, Y. Zhou, J. Neu, M. Worku, E. Berkwits, Q. Q. He, S. Lee, X. S. Lin, T. Siegrist, M. H. Du and B. W. Ma, *ACS Materials Lett.*, 2019, **1**, 594-598.
2. V. Morad, Y. Shynkarenko, S. Yakunin, A. Brumberg, R. D. Schaller and M. V. Kovalenko, *J. Am. Chem. Soc.*, 2019, **141**, 9764-9768.
3. C. K. Zhou, H. R. Lin, M. Worku, J. Neu, Y. Zhou, Y. Tian, S. Lee, P. Djurovich, T. Siegrist and B. W. Ma, *J. Am. Chem. Soc.*, 2018, **140**, 13181–13184.
4. C. K. Zhou, H. R. Lin, H. L. Shi, Y. Tian, C. Pak, M. Shatruk, Y. Zhou, P. Djurovich, M. H. Du and B. W. Ma, *Angew. Chem. Int. Ed.*, 2018, **130**, 1033-1036.
5. C. K. Zhou, Y. Tian, M. C. Wang, A. Rose, T. Besara, N. K. Doyle, Z. Yuan, J. C. Wang, R. Clark, Y. Y. Hu, T. Siegrist, S. C. Lin and B. W. Ma, *Angew. Chem. Int. Ed.*, 2017, **56**, 9018-9022.
6. C. K. Zhou, H. R. Lin, Y. Tian, Z. Yuan, R. Clark, B. H. Chen, L. J. van de Burgt, J. C. Wang, Y. Zhou, K. Hanson, Q. J. Meisner, J. Neu, T. Besara, T. Siegrist, E. Lambers, P. Djurovich and B. W. Ma, *Chem. Sci.*, 2018, **9**, 586-593.
7. D. Han, H. L. Shi, W. M. Ming, C. K. Zhou, B. W. Ma, B. Saparov, Y. Z. Ma, S. Y. Chen and M. H. Du, *J. Mater. Chem. C.*, 2018, **6**, 6398-6405.
8. C. K. Zhou, M. Worku, J. Neu, H. R. Lin, Y. Tian, S. Lee, Y. Zhou, D. Han, S. Y. Chen, A. Hao, P. I. Djurovich, T. Siegrist, M. H. Du and B. W. Ma, *Chem. Mater.*, 2018, **30**, 2374–2378.
9. S. Lee, C. K. Zhou, J. Neu, D. Beery, A. Arcidiacono, M. Chaaban, H. R. Lin, A. Gaiser, B. H. Chen, T. E. Albrecht-Schmitt, T. Siegrist and B. W. Ma, *Chem. Mater.*, 2020, **32**, 374-380.
10. D. Chen, S. Q. Hao, G. J. Zhou, C. K. Deng, Q. L. Liu, S. L. Ma, C. Wolverton, J. Zhao and Z. G. Xia, *Inorg. Chem.*, 2019, **58**, 15602-15609.
11. L. Zhou, J. F. Liao, Z. G. Huang, J. H. Wei, X. D. Wang, H. Y. Chen and D. B. Kuang, *Angew. Chem. Int. Ed.*, 2019, **58**, 15435-15440.
12. L. Zhou, J. F. Liao, Z. G. Huang, J. H. Wei, X. D. Wang, W. G. Li, H. Y. Chen, D. B. Kuang, C. Y. Su, *Angew. Chem. Int. Ed.*, 2019, **58**, 5277-5281.